

## The Crystal Structure of Maucherite ( $\text{Ni}_{11}\text{As}_8$ )

MICHAEL E. FLEET

Department of Geology, University of Western Ontario, London, Ontario, Canada

### Abstract

X-ray diffraction patterns of maucherite ( $\text{Ni}_{11}\text{As}_8$ ) indicate the presence of a tetragonal supercell with  $a = 6.8724(4)$  Å,  $c = 21.821(1)$  Å, space group  $P4_21_2$ ,  $Z = 4$ ; the subcell is also tetragonal with  $a' = a/2$ ,  $c' = c$ , space group  $I4_1/amd$ ,  $Z = 1$ . The crystal structure has been determined using X-ray intensity data collected from a synthetic maucherite crystal on a four-circle diffractometer and refined to an  $R$  value of 0.063. The structure contains six non-equivalent Ni atoms per unit cell, five in square pyramidal coordination with As in equipoint position  $8b$  and one in a stretched octahedral coordination in equipoint position  $4a$ . The As polyhedra form single chains of trigonal prisms arranged so that the prism faces contribute to the square pyramidal Ni sites. Alternate prisms share a face with a prism from an adjacent chain; the site which includes the shared face is vacant to account for the unusual stoichiometry of maucherite. Each Ni is coordinated to four or five neighboring Ni atoms with Ni-Ni distances of 2.48 Å to 2.87 Å. The shorter distances arise through shared pyramidal faces and shared As polyhedral prisms; the longer ones arise through shared pyramidal-octahedral faces and shared pyramidal edges. It is suggested that  $3d$  electron  $\sigma$  bonding between these related Ni atoms supplements the Ni-As  $\sigma$  bonds. The principal features of the maucherite structure have counterparts in the crystal structures of  $\alpha$ - $\text{Ni}_7\text{S}_6$  and millerite ( $\text{NiS}$ ).

### Introduction

Maucherite ( $\text{Ni}_{11}\text{As}_8$ ) is found associated with niccolite ( $\text{NiAs}$ ), rammelsbergite ( $\text{NiAs}_2$ ) and parammelsbergite ( $\text{NiAs}_2$ ) in nickel-cobalt-native silver deposits as exemplified at Eisleben, Thuringia, Germany (the type locality) and Cobalt, Ontario, Canada.

Most of the present crystallographic data on maucherite were obtained by Peacock (1940) who, confirming earlier work by Laves (1935), reported that single crystal X-ray diffraction patterns indicate a well-developed pseudocell (subcell) which is tetragonal with  $a = 3.42$  Å,  $c = 21.83$  Å and space group  $I4_1/amd$  ( $D_{4h}^{19}$ ) but that the real unit cell, also tetragonal, is defined by a doubling of the  $a$ -axis, giving  $a = 6.84$  Å,  $c = 21.83$  Å, space group  $P4_12_12$  ( $D_4^4$ ) or  $P4_32_12$  ( $D_4^8$ ). However, the reflections characteristic of the supercell are diffuse and smeared into  $hk$  bands of continuous radiation (Peacock, 1942). On the basis of chemical analyses of several natural samples, Peacock (1940) established the composition as  $\text{Ni}_{11}\text{As}_8$ ; small amounts of Co and S substitute for Ni and As respectively. A measured density of  $8.00 \text{ gm cm}^{-3}$  indicated  $Z = 4$ , and Peacock argued that the structure must contain four vacancies in the Ni sites per unit cell.

Laves (1935) showed that a synthetic  $\text{Ni}_3\text{As}_2$  composition was crystallographically equivalent to maucherite, but systematic phase chemistry on the binary system later indicated that the stability region of synthetic maucherite was very narrow and restricted to  $\text{Ni}_{11}\text{As}_8$  (Heyding and Calvert, 1957). Yund (1961) confirmed the chemical and crystallographic equivalence of natural maucherite and the synthetic phase synthesized below  $700^\circ\text{C}$ . X-ray powder diffraction patterns of the product quenched from above  $700^\circ\text{C}$  contain several additional reflections; however, a phase transition in the temperature range  $650^\circ$  to  $800^\circ\text{C}$  was not indicated by differential thermal analyses.  $\text{Ni}_{11}\text{As}_8$  melts incongruently at  $830^\circ \pm 5^\circ\text{C}$  to niccolite plus liquid.

### Experimental

A crystal structure determination on natural maucherite was not possible because of the diffuse nature of the superstructure reflections in all the specimens examined to date. Thus it was decided to attempt synthesis of a maucherite in which these reflections were sharp. Clearly, the existence of the diffuse reflections in the natural product indicates that maucherite attempts further long-range order at low temperatures, so that the synthetic material should be annealed at a temperature higher than that at which this long-range order is initiated but at or below  $700^\circ\text{C}$  to prevent the formation of the possible metastable phase reported by Yund (1961).

About 1.0 gm of  $\text{Ni}_{11}\text{As}_8$  was synthesized by heating an appropriate mixture of purified Ni sponge, previously reduced with hydrogen at  $900^\circ\text{C}$ , and As powder in an evacuated silica-glass tube placed in a horizontal tube furnace. Initially, the charge was heated at  $795^\circ\text{C}$  for 11 days to attempt complete reaction of the starting reactants, then annealed at  $696^\circ\text{C}$  for five days. However, the product contained NiAs and Ni in addition to  $\text{Ni}_{11}\text{As}_8$ . Homogenization was completed by preparing a second charge from the ground products of the first synthesis and heating this at  $825^\circ\text{C}$  for one day, and  $790^\circ\text{C}$  for six days, then annealing it at  $692^\circ\text{C}$  for three days. The charge was allowed to cool to room temperature in the furnace. The product of the synthesis was massive and in the form of a plug. This was crushed in a percussion mortar and fragments within the size range 0.01 mm to 0.2 mm in diameter were isolated by sieving. The material appeared homogeneous in polished section examination and the individual fragments were generally monocrystalline. The crystal fragment selected for study was bounded by plane surfaces, with a near-rhombic habit, and had a calculated volume of  $0.1 \times 10^{-6} \text{ cm}^3$ .

A preliminary single crystal study on a precession camera confirmed the fragment to be a single crystal with reflections characteristic of the supercell sharp and distinct. The existing crystallographic data on maucherite were confirmed also: the subcell is tetragonal with the systematic absences  $hkl$  with  $h+k+l \neq 2n$ ,  $hk0$  with  $h \neq 2n$  and  $hhl$  with  $2h + l \neq 4n$ , consistent with the space group  $I4_1/amd$  ( $D_{4h}^{19}$ ), and the supercell is tetragonal with the systematic absences  $00l$  with  $l \neq 4n$  and  $h00$  with  $h \neq 2n$ , consistent with the enantiomorphic space groups  $P4_12_12_1$  ( $D_4^4$ ) and  $P4_32_12_1$  ( $D_4^8$ ). The lattice parameters of the supercell, determined by least-squares refinement of 12 centered reflections measured on a four-circle diffractometer with Zr-filtered  $\text{MoK}\alpha$  ( $\lambda = 0.7107 \text{ \AA}$ ) radiation, are  $a = 6.8724(4) \text{ \AA}$ ,  $c = 21.821(1) \text{ \AA}$ . These data compare quite well with the parameters reported by Heyding and Calvert (1957;  $a = 6.868(4) \text{ \AA}$ ,  $c = 21.80(2) \text{ \AA}$ ) and Yund (1961;  $a = 6.867(2) \text{ \AA}$ ,  $c = 21.80(1) \text{ \AA}$ ) for synthetic maucherite, both sets of data being determined from powder patterns.

The X-ray intensity data for the structure analysis were taken on a Picker FACS 1 four-circle diffractometer system at the University of Western Ontario. All non-equivalent  $hkl$  reflections with  $2\theta \leq 65^\circ$  were measured using a scintillation detector, Zr-filtered  $\text{MoK}\alpha$  ( $\lambda = 0.7107 \text{ \AA}$ ) radiation and the  $2\theta$  scan technique: 40 second stationary background counts, peak-base widths of  $2.0^\circ 2\theta$  (uncorrected for dispersion) and a scanning rate of  $0.5^\circ$  per minute. The resulting data were processed by a data correction routine which corrected for background, Lorentz and polarization effects, and absorption. Transmission factors for the absorption correction were calculated by the analytical method of de Meulenaer and Tompa (1965) using a value for the linear absorption coefficient of  $463.5 \text{ cm}^{-1}$ . The crystal was oriented with the  $a$ -axis parallel to the  $\phi$  axis. The calculated transmission factors varied from 0.14 for 017 to 0.20 for 021. Standard deviations ( $\sigma$ ) were calculated from the expression  $\sigma = 1/2 [1/LpT \cdot (\sigma_p^2 + \sigma_{b1}^2 + \sigma_{b2}^2 + (0.02I)^2)/I]^{1/2}$ , where  $Lp$  is the Lorentz-polar-

ization factor,  $T$  is the transmission factor,  $\sigma_p$ ,  $\sigma_{b1}$  and  $\sigma_{b2}$  are, respectively, the standard deviations for the counting rates of the peak and backgrounds and  $I$  is the background-corrected peak intensity. Each reflection whose intensity was less than the associated background plus  $3\sigma$  was given zero intensity. The final data list contained 1178 reflections of which 713 were 'unobserved.' The large number of 'unobserved' reflections is attributed to the manner in which the superstructure is developed from the substructure; there is, for example, a structural extinction for  $hkl$  with  $h \neq 2n$  and  $h + k = 2n$ .

### Crystal Structure Investigation

The true cell of maucherite is defined by a non-centrosymmetric superstructure. The crystal structure investigation was initiated by a determination of the structure of the subcell, in the expectation that the positional data for the disordered basic structure could be expanded into an ordered arrangement which would account for the X-ray diffraction intensity distribution of the supercell.

The crystal structure of the subcell is centrosymmetric; the space group  $I4_1/amd$  being uniquely defined by the systematic absences. The structure factors were converted to normalized structure factors ( $E$ 's) using program FAME (R. B. K. Dewar, Illinois Institute of Technology, Chicago) and the phases of those normalized structure factors with  $E \geq 1.5$  were assigned by a reiterative application of Sayre's equation using program REL1 (adapted from Long, 1965, and further modified by the author to accommodate space group  $I4_1/amd$ ). Atomic positions taken from  $E$  maps, prepared from the solution with the largest consistency index (0.81), lead directly to a value of the conventional residual index of 0.30.

The structure was improved following an  $F_0$  Fourier analysis and refined further by full-matrix, least-squares refinement using program RFINE (L. Finger, Geophysical Laboratory, Washington), which minimizes the function  $\sum w (|F_0| - |F_c|)^2$ , where  $w = 1/\sigma^2$ ,  $F_0$  is the observed and  $F_c$  the calculated structure factor, and calculates a conventional residual index,  $\sum ||F_0| - |F_c|| / \sum |F_0|$  and a weighted residual index,  $[\sum w (|F_0| - |F_c|)^2 / \sum w F_0^2]^{1/2}$ . The scattering curves for  $\text{Ni}^{2+}$  and As were taken from Cromer and Mann (1968) and real and imaginary components of the anomalous dispersion coefficients for Ni and As were from Cromer (1965). The refinement converged, giving values of the conventional and weighted residual indices of 0.047 and 0.053; the final positional and isotropic thermal parameters are given in Table 1.

The unit cell content of the subcell is  $\text{Ni}_{11}\text{As}_8$ . The

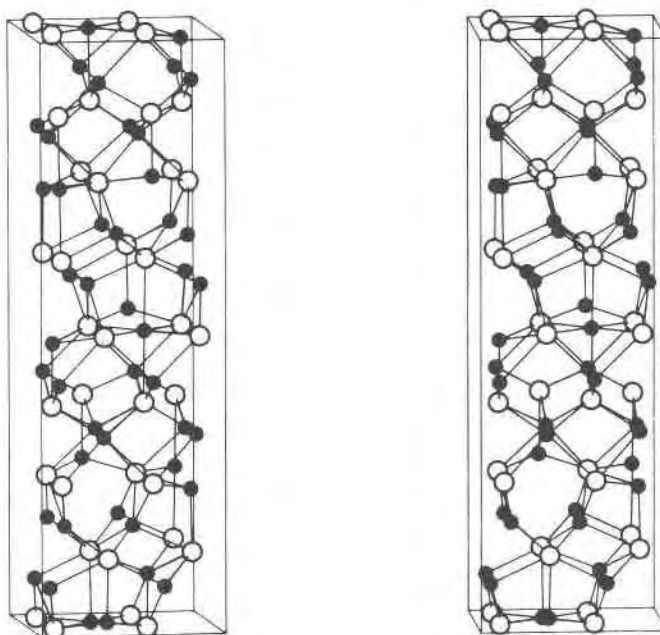


FIG. 1. Stereoscopic view of the crystal structure of maucherite; Ni: small full circles. As: large open circles.

structure analysis has shown that four As are ordered in the As(1) sites and that the remaining four As are disordered among the As(2) sites, with an occupancy of 0.5. All of the Ni are in disordered positions, with eight Ni in Ni(3) sites, occupancy 0.5, two Ni in Ni(1) sites, occupancy 0.25, and one Ni in Ni(2) sites, occupancy 0.25.

The crystal structure of the superstructure was developed by expanding the positional data of the subcell, with a suitable change in origin, to conform to the non-centrosymmetric space group  $P4_12_12$ . Initially, several trial structures giving reasonable Ni coordinations with unit site occupancies were attempted. Comparison of these resulted in a set of ordered sites which satisfied the general features of the diffraction intensity distribution of the supercell. The agreement between the observed and calculated structure factors was improved following analysis of

$F_0$  Fourier maps. These ordered sites and the subcell sites they are related to are given in Table 2. The superstructure contains six non-equivalent Ni atoms per unit cell of which five, Ni(1), Ni(3), Ni(4), Ni(5) and Ni(6) in 8b equipoint positions, are in square pyramidal coordination with As, and one, Ni(2) in 4a, is in a stretched octahedral coordination with As (Fig. 1). The As polyhedra form single chains of trigonal prisms arranged so that the prism faces contribute to the square pyramidal Ni sites (Fig. 2).

The positional and thermal parameters were refined using program RFINE. Initially, constraints were added to relate the parameters of Ni(4), Ni(5), and Ni(6) to those of Ni(3), of As(2) and As(3) to

TABLE 1. Positional and Thermal Parameter for Subcell\*

TABLE 1. POSITIONAL AND THERMAL PARAMETERS FOR SUBCELL*							
Site	Equipoint position	Site occupancy	x	y	z	B	
Ni(1)	8e	0.25	0	3/4	0.1076(6)	0.64(17)	
Ni(2)	4a	0.25	0	3/4	1/8	0.98(39)	
Ni(3)	16h	0.5	0	0.1292(9)	0.2033(1)	0.44(5)	
As(1)	4b	1.0	0	1/4	3/8	0.46(5)	
As(2)	8e	0.5	0	1/4	0.9980(2)	0.39(6)	

\*Estimated standard deviations (in parentheses) refer to the last decimal place cited. Thus 0.64(17) means an *esd* of 0.17 whereas 0.1076(6) indicates an *esd* of 0.0006.

TABLE 2. Approximate Positional Parameters for Maucherite

TABLE 2. APPROXIMATE POSITIONAL PARAMETERS FOR MAUCHERITE					
Site	Equivalent subcell site	Equipoint position	x	y	z
Ni(1)	Ni(1)	8b	1/8	3/8	0.269
Ni(2)	Ni(2)	4a	3/8	3/8	0
Ni(3)	Ni(3)	8b	1/8	0.565	0.172
Ni(4)	Ni(3)	8b	5/8	0.565	0.172
Ni(5)	Ni(3)	8b	3/8	0.685	0.078
Ni(6)	Ni(3)	8b	7/8	0.685	0.078
As(1)	As(1)	4a	1/8	1/8	0
As(2)	As(1)	4a	5/8	5/8	0
As(3)	As(1)	8b	5/8	1/8	0.0
As(4)	As(2)	8b	7/8	3/8	0.123
As(5)	As(2)	8b	1/8	7/8	0.127

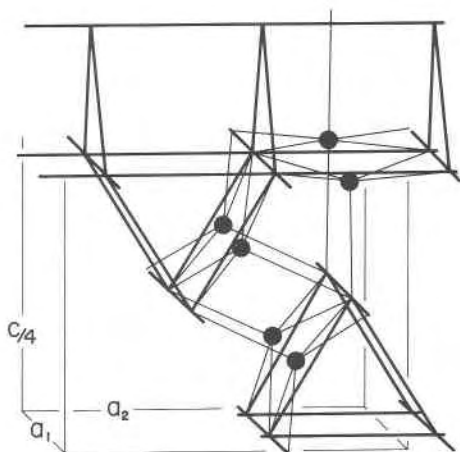


FIG. 2. Intersecting chains of trigonal prisms of As atoms in the maucherite structure; Ni: small full circles.

those of As(1), and of As(5) to those of As(4) (Table 2). The values of the conventional and weighted residual indices thus obtained for isotropic thermal motion are 0.130 and 0.098 respectively. The refinement was continued by removing the inter-site positional constraints and finally converged on values of the conventional and weighted residual indices of 0.078 and 0.063 respectively. Convergence was assumed when the changes to the positional parameters were in the sixth places and the changes in the thermal parameters were in the fifth places and the ratios of the changes in the parameters to the errors in the parameters were less than 0.005. The positional and isotropic thermal parameters are given in Table 3, and the observed and calculated structure factors are given in Table 4. The isotropic thermal parameters were constrained as in the initial stage of the refinement. In unconstrained refinement

TABLE 3. Refined Positional and Thermal Parameters for Maucherite\*

Site	x	y	z	B
Ni(1)	0.125(2)	0.373(2)	0.2686(3)	0.66(9)
Ni(2)	3/8	3/8	0	0.43(13)
Ni(3)	0.120(3)	0.569(2)	0.1734(4)	0.35(4)
Ni(4)	0.608(2)	0.562(2)	0.1710(5)	0.35(4)
Ni(5)	0.372(3)	0.683(2)	0.0805(4)	0.35(4)
Ni(6)	0.871(3)	0.690(2)	0.0770(4)	0.35(4)
As(1)	0.120(2)	0.120(2)	0	0.43(5)
As(2)	0.635(2)	0.635(2)	0	0.43(5)
As(3)	0.635(2)	0.129(2)	0.0004(2)	0.43(5)
As(4)	0.877(2)	0.382(2)	0.1250(2)	0.32(5)
As(5)	0.121(2)	0.869(2)	0.1289(2)	0.32(5)

\*Standard deviations in parentheses

the thermal parameter of Ni(3) and Ni(6) refined to negative values. Attempts at constrained anisotropic refinement resulted in negative  $B_{33}$  parameters for Ni(3) and Ni(6). Furthermore, the motions of the remaining atoms were virtually isotropic and the reductions in the residual indices were not significant. The correlation coefficients for those positional parameters related through common subcell sites are given in Table 5 and indicate a high interdependency for these parameters.

### Discussion

The crystal structure of maucherite has a substructure of As polyhedra in the form of single chains of trigonal prisms arranged so that alternate prisms share a face with a prism from an adjacent chain (Fig. 2). The shared faces lie in planes normal to the  $c$ -axis at  $z = 0, 1/4, 1/2$  and  $3/4$ . The 44 Ni atoms per unit cell are accommodated in six non-equivalent positions, five in square pyramidal coordination with As and one in a stretched octahedral coordination with As. There are 40 unshared prism faces of the As polyhedra per unit cell and each of these contributes to the square pyramidal sites so that the base of each square pyramid is formed on one As polyhedral unit and the apex is formed on a neighboring unit. The four octahedral sites per unit cell are formed from a square planar arrangement of As within the planes of shared prism faces, at  $z = 0, 1/4, 1/2$  and  $3/4$ , and from more distant As in polyhedral units immediately above and below these planes. The possible metal sites formed about the shared faces themselves are vacant. Thus, the 44 Ni atoms per unit cell are located in 44 discrete structural positions. The structure specifically accommodates the composition of the compound,  $Ni_{11}As_8$ , and is not a non-stoichiometric variant of an established or hypothetical  $A_3B_2$  structure as suggested earlier (Peacock, 1940). The establishment of  $Ni_{11}As_8$  as a stoichiometric compound largely accounts for its restricted range in composition (Yund, 1961).

Some relevant interatomic distances and bond angles are given in Table 6 and 7 respectively (the atom identification labels are consistent with the usage in Figure 3; atoms marked by an asterisk are located in adjacent unit cells). The Ni-As bond distances range from 2.28 Å to 2.54 Å; the stretched Ni-As bond distance in the octahedral site is 2.64 Å. The shorter distances tend to be to the apical As in the square pyramidal coordinations. These values may be compared to a Ni-As bond distance of 2.439



TABLE 5. Correlation Coefficients ( $r$ ) for Related Superstructure Positional Parameters

	$r$	$r$	$r$
	<b>x-Ni(3)</b>	<b>x-Ni(4)</b>	<b>x-Ni(5)</b>
x-Ni(4)	0.121		
x-Ni(5)	-0.204	0.409	
x-Ni(6)	0.553	0.032	0.384
	<b>y-Ni(3)</b>	<b>y-Ni(4)</b>	<b>y-Ni(5)</b>
y-Ni(4)	-0.735		
y-Ni(5)	0.661	-0.547	
y-Ni(6)	-0.547	0.657	-0.746
	<b>z-Ni(3)</b>	<b>z-Ni(4)</b>	<b>z-Ni(5)</b>
z-Ni(4)	-0.511		
z-Ni(5)	-0.561	0.271	
z-Ni(6)	0.282	-0.582	-0.513
	<b>x-As(1)</b>	<b>x-As(2)</b>	<b>x-As(3)</b>
x-As(2)	-0.005		
x-As(3)	0.444	-0.437	
y-As(3)	-0.385	0.336	0.193
	<b>x-As(4)</b>	<b>y-As(4)</b>	<b>x-As(5)</b>
y-As(4)	0.114		
x-As(5)	-0.813	-0.047	
y-As(5)	-0.152	-0.631	0.126
	<b>z-As(4)</b>		
z-As(5)	0.490		

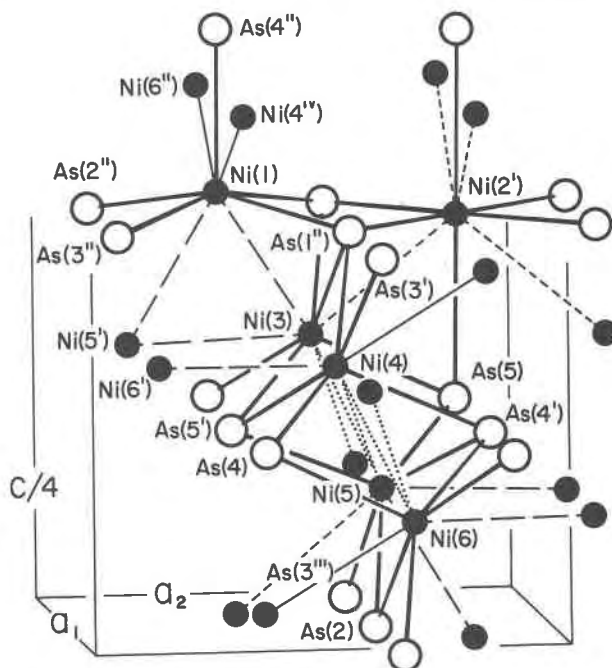


FIG. 3. Nearest-neighbor Ni environments in maucherite; Ni-Ni bonds indicated by shared pyramidal faces: full lines; shared trigonal prisms of As atoms: long dashes; shared pyramidal-octahedral faces: short dashes; shared pyramidal edges: stipples.

TABLE 6. Interatomic Distances in Maucherite

Atoms*	Distance (Å)**	Atoms*	Distance (Å)**
Ni(1) - As(1 <sup>1'</sup> )	2.47(1)	As(1 <sup>1'</sup> ) - As*(3 <sup>1'</sup> )	3.54(1)
- As*(2 <sup>1'</sup> )	2.46(1)	- As(3 <sup>1'</sup> )	3.335(0)
- As*(3 <sup>1'</sup> )	2.54(2)	- As(4 <sup>1'</sup> )	3.668(7)
- As(3 <sup>1'</sup> )	2.39(2)	As*(2 <sup>1'</sup> ) - As*(3 <sup>1'</sup> )	3.39(2)
- As(4 <sup>1'</sup> )	2.322(5)	- As(3 <sup>1'</sup> )	3.48(2)
		- As(4 <sup>1'</sup> )	3.639(6)
Ni(2 <sup>1'</sup> ) - As(1 <sup>1'</sup> )	2.48(1)	As*(3 <sup>1'</sup> ) - As(4 <sup>1'</sup> )	3.67(1)
- As*(2 <sup>1'</sup> )	2.524(9)	As(3 <sup>1'</sup> ) - As(4 <sup>1'</sup> )	3.63(1)
- As*(3 <sup>1'</sup> )	2.46(1)	As(1 <sup>1'</sup> ) - As(5)	3.62(1)
- As(5)	2.643(5)	As*(2 <sup>1'</sup> ) - As*(3 <sup>1'</sup> )	3.48(2)
		- As(5)	3.66(1)
Ni(3) - As(1 <sup>1'</sup> )	2.47(2)	As*(3 <sup>1'</sup> ) - As(5)	3.57(1)
- As*(3 <sup>1'</sup> )	2.45(1)	As(1 <sup>1'</sup> ) - As(5)	3.62(1)
- As*(4)	2.36(2)	As*(2 <sup>1'</sup> ) - As*(3 <sup>1'</sup> )	3.48(2)
- As(5)	2.28(1)	- As(5)	3.66(1)
- As(5 <sup>1'</sup> )	2.52(2)		
Ni(4) - As(1 <sup>1'</sup> )	2.36(1)	As*(3 <sup>1'</sup> ) - As(5)	3.57(1)
- As*(3 <sup>1'</sup> )	2.51(1)	As(3 <sup>1'</sup> ) - As(5)	3.65(1)
- As(4)	2.44(1)	As(1 <sup>1'</sup> ) - As(5 <sup>1'</sup> )	3.30(1)
- As(4 <sup>1'</sup> )	2.42(1)		
- As(5 <sup>1'</sup> )	2.33(1)	As(5) - As(5 <sup>1'</sup> )	3.87(2)
Ni(5) - As(2)	2.54(1)	As(1 <sup>1'</sup> ) - As(3 <sup>1'</sup> )	3.34(1)
- As*(3 <sup>1''')</sup> )	2.46(2)	As(5) - As(4 <sup>1'</sup> )	3.668(7)
- As(4)	2.40(2)	As(3 <sup>1'</sup> ) - As(4)	3.21(1)
- As(5)	2.39(2)	- As(4 <sup>1'</sup> )	3.63(1)
- As(5 <sup>1'</sup> )	2.33(1)	As(4) - As(4 <sup>1'</sup> )	3.86(2)
		As(4) - As(5 <sup>1'</sup> )	3.426(0)
Ni(6) - As(2)	2.37(2)	As(4 <sup>1'</sup> ) - As(5 <sup>1'</sup> )	3.90(2)
- As*(3 <sup>1''')</sup> )	2.47(2)	As(2) - As*(3 <sup>1''')</sup> )	3.48(2)
- As(4)	2.36(1)	- As(4 <sup>1'</sup> )	3.214(9)
- As(4 <sup>1'</sup> )	2.40(2)	- As(5 <sup>1'</sup> )	3.66(1)
- As*(5)	2.40(2)		
Ni(1) - Ni(3)	2.48(1)	As*(3 <sup>1''')</sup> ) - As(4)	3.67(1)
- Ni(4 <sup>v</sup> )	2.53(2)	As(4) - As*(5)	3.75(2)
- Ni(5 <sup>1'</sup> )	2.53(1)		
- Ni(6 <sup>1''')</sup> )	2.51(2)		
Ni(2 <sup>1'</sup> ) - Ni(3)	2.69(1)		
- Ni*(5 <sup>1'</sup> )	2.75(1)	As(3 <sup>1''')</sup> ) - As(5)	3.25(1)
		As(2) - As*(3 <sup>1''')</sup> )	3.39(2)
Ni(3) - Ni(5)	2.79(2)	- As(4)	3.639(6)
- Ni(5 <sup>1'</sup> )	2.65(2)		
- Ni*(6)	2.835(7)		
		As*(3 <sup>1''')</sup> ) - As(4)	3.67(1)
Ni(4) - Ni(5)	2.688(8)	As(4) - As*(5)	3.75(2)
- Ni(6)	2.87(1)		
- Ni(6 <sup>1'</sup> )	2.56(2)		

\*Atoms marked by asterisks are located in adjacent unit cells  
 \*\*Standard deviations (in parentheses) refer to the last decimal place cited

orthorhombic structure of  $\alpha$ -Ni<sub>7</sub>S<sub>6</sub> is more complex. The Ni is distributed among five non-equivalent sites. These include one tetrahedral site, with a site occupancy of approximately 0.5, and four square pyramidal sites, two with site occupancies of approximately 1.0 and two with site occupancies of approximately 0.5 (Fleet, 1972a). Twelve of the 20 S atoms per unit cell are organized into chains of trigonal prisms parallel to the  $a$ -axis at  $y = 1/4$  and  $3/4$ . The prism faces contribute to the two square pyramidal sites which have near unit occupancy. Each Ni site has several possible Ni neighbors: the Ni atoms in square pyramidal coordination are related through shared pyramidal faces, shared trigonal prisms of S, and shared pyramidal edges, so that, as in the maucherite structure, there is a range of observed Ni-Ni distances, from 2.457 Å to 2.849 Å.

During the early stages of this investigation, a

TABLE 7. Bond Angles in Maucherite

Atoms* forming angle	Angle**	Atoms* forming angle	Angle**
As(1'')-Ni(1)-As*(2'')	161.0(3)°	As(1'')-Ni(4)-As(3')	86.4(5)°
-As*(3')	89.9(5)	-As(4)	152.6(7)
-As(3'')	86.6(5)	-As(4')	100.1(6)
-As(4'')	99.8(4)	-As(5')	89.4(5)
As*(2'')-Ni(1)-As*(3')	85.6(6)	As(3')-Ni(4)-As(4)	80.8(5)
-As(3'')	91.7(5)	-As(4')	95.0(6)
-As(4'')	99.1(4)	-As(5')	154.4(7)
As*(3')-Ni(1)-As(3'')	161.0(3)	As(4)-Ni(4)-As(4')	105.0(4)
-As(4'')	98.2(5)	-As(5')	91.9(3)
As(3'')-Ni(1)-As(4'')	100.8(5)	As(4')-Ni(4)-As(5')	110.6(5)
As(1'')-Ni(2')-As*(2'')	180.0(0)	As(2)-Ni(5)-As(3''')	88.2(5)
-As*(3')	91.5(4)	-As(4')	81.1(7)
-As(5)	89.8(3)	-As(5)	152.6(6)
As*(2'')-Ni(2')-As*(3')	88.5(4)	-As(5')	97.3(6)
-As(5)	90.2(3)	As(3''')-Ni(5)-As(4')	149.0(6)
As*(3')-Ni(2')-As*(3''')	177.0(7)	-As(5)	84.2(7)
-As(5)	88.8(3)	-As(5')	99.2(7)
As*(3'')-Ni(2')-As(5)	91.3(3)	As(4')-Ni(5)-As(5)	92.1(4)
As(5)-Ni(2')-As(5'v)	179.6(5)	-As(5')	111.0(7)
As(1'')-Ni(3)-As*(3')	91.9(4)	As(5)-Ni(5)-As(5')	109.9(6)
-As*(4)	153.1(6)	As(2)-Ni(6)-As*(3''')	89.0(4)
-As(5)	99.1(7)	-As(4')	100.6(7)
-As(5')	82.7(7)	-As(4)	84.8(7)
As*(3')-Ni(3)-As*(4)	83.7(7)	-As(5)	155.3(7)
-As(5)	98.0(7)	As*(3''')-Ni(6)-As(4)	98.8(6)
-As(5')	154.6(6)	-As(4')	153.0(6)
As*(4)-Ni(3)-As(5)	107.8(7)	-As*(5)	83.6(8)
-As(5')	90.0(4)	As(4)-Ni(6)-As(4')	108.2(6)
As(5)-Ni(3)-As(5')	107.5(5)°	-As*(5)	103.8(6)
		As(4')-Ni(6)-As*(5)	91.1(4)°

\*Atoms marked by asterisks are located in adjacent unit cells.

\*\*Standard deviations (in parentheses) refer to the last decimal place cited.

specimen of natural maucherite from Eisleben, Thuringia, was examined, although the examination was limited by an inability to obtain single crystal fragments. The virtual crystallographic equivalence of synthetic  $\text{Ni}_{11}\text{As}_8$  and natural maucherite was confirmed. Also, in agreement with earlier workers (Peacock, 1940; Jagodzinski and Laves, 1948),  $0kl$  superstructure reflections are smeared in the  $c^*$ -axis direction. However, the diffraction maxima are centered in the same relative positions and are of the same relative intensity as in the synthetic product. In addition, the  $hk0$  superstructure reflections are replaced by diffuse areas of satellite diffraction in the form of small crosses centered on the positions of the original reflections.

The diffuse satellite reflections indicate that maucherite attempts further long-range ordering processes at low temperature, the full development of which is inhibited by very slow reaction rates. The ordering may be due to a modulation of the structure. However, this modulation cannot be unidirectional in the  $c$ -axis direction, since satellite reflections are observed for  $hk0$  reflections as well as for

$0kl$  reflections. The diffuse nature of the satellite reflections suggests that the modulation must have a variable periodicity. It is difficult to predict the actual structural expression of the ordering, although one might expect a further rationalization of the Ni-Ni interactions involving, in part, the development of two square pyramidal sites from the stretched octahedral site of the Ni(2) atoms, one site being occupied in any instance and the modulation being based on the sequence of occupancy of the two sites.

The unit cell composition of maucherite is  $\text{Ni}_{44}\text{As}_{32}$ . The structure requires 224 Ni-As  $\sigma$  bonds per unit cell; compared to the assumed single Ni-As bond distances for octahedral coordination in paramelsbergite, most of these  $\sigma$  bonds must have either unit or near-unit bond numbers. The outer electron configuration of Ni is  $3d^84s^2$  and that of As is  $4s^24p^3$ . The molecular orbital bonding theory would require that the  $4s$  electrons on the Ni atoms and the  $4s$  and  $4p$  electrons on the As contribute to the Ni-As  $\sigma$  bonding scheme; these total 248 electrons per unit cell, far fewer than required for 224 full  $\sigma$  bonds. The remaining electrons must be supplied by the  $3d$  electrons on the Ni atoms. Of these, the  $d_{xy}$ ,  $d_{xz}$  and  $d_{yz}$  orbitals are poorly disposed to contribute to the Ni-As  $\sigma$  bonds, and the  $3d$  electron contribution can be made only via the axially oriented  $d_{x^2-y^2}$  and  $d_{z^2}$  orbitals. On the isolated atom these are doubly degenerate and carry one electron each. However, in maucherite the short Ni-Ni distances indicate strong positive interactions between the  $d_{xy}$ ,  $d_{xz}$  and  $d_{yz}$  orbitals which project through the pyramidal and octahedral edges. The interaction of the orbitals projected between the Ni atoms related through shared pyramidal edges will be  $\sigma$  bonding in character since the orbitals overlap end-on. However, orbitals between the Ni atoms related through shared pyramidal faces, shared trigonal prisms of As atoms, and shared pyramidal-octahedral faces will interact obliquely. Although the site symmetries of the Ni atoms related by shared trigonal prisms of As atoms would permit  $\pi$  bonding between those orbitals normal to the bonding plane,  $\pi$  bonding possibilities for the other Ni-Ni bonds are limited. It seems logical, then, to argue that, as in parkerite ( $\text{Ni}_3\text{Bi}_2\text{S}_2$ ) where the Ni atoms are related at moderately short distances through shared octahedral faces (Fleet, unpublished data), all of the  $d_{xy}$ ,  $d_{xz}$  and  $d_{yz}$  orbital interactions are  $\sigma$  bonding in character, the oblique orbital interactions giving rise to fractional bent  $\sigma$  bonds. Alternatively, one might invoke a hybridization of

these orbitals on each Ni to allow direct bonding orbitals between the related Ni atoms. The  $d_{xy}$ ,  $d_{yz}$  and  $d_{zx}$  orbitals are triply degenerate on the isolated atom and carry two electrons each, but a  $\sigma$  bonding role must require fewer electrons. If, say, two of these are added to the  $d_{x^2-y^2}$  and  $d_{z^2}$  orbitals, allowing a maximum contribution of four  $3d$  electrons per Ni atom to the Ni-As  $\sigma$  bonds, the remaining four  $3d$  electrons may be distributed among the bonding and antibonding Ni-Ni  $\sigma$  orbitals such that for the shorter Ni-Ni bonds, which are similar to the bond distance in metallic Ni (2.492 Å), a greater proportion would be bonding and for the longer distances relatively more would be antibonding. There are now 424 electrons for the Ni-As  $\sigma$  bonds; the discrepancy of 24 electrons per unit cell must reflect some degree of partial bond formation; for example, the stretched Ni(2)-As(5) bonds would represent bond numbers of about 0.5.

#### Acknowledgments

This work was supported by a National Research Council of Canada operating grant.

#### References

- CROMER, D. T. (1965) Anomalous dispersion corrections computed from self-consistent field relativistic Dirac-Slater wave functions. *Acta Crystallogr.* **18**, 17-23.
- , AND J. B. MANN (1968) X-ray scattering factors computed from numerical Hartree-Fock wave functions. *Acta Crystallogr.* **A24**, 321-323.
- DE MEULENAER, J., AND H. TOMPA (1965) The absorption correction in crystal structure analysis. *Acta Crystallogr.* **19**, 1014-1018.
- FLEET, M. E. (1972a) The crystal structure of  $\alpha$ -Ni<sub>2</sub>Se. *Acta Crystallogr.* **B28**, 1237-1241.
- (1972b) The crystal structure of parammelsbergite (NiAs<sub>2</sub>). *Amer. Mineral.* **57**, 1-9.
- HEYDING, R. D., AND L. D. CALVERT (1957) Arsenides of the transition metals. II. The nickel arsenides. *Can. J. Chem.* **35**, 1202-1215.
- JAGODZINSKI, H., AND F. LAVES (1948) Eindimensionale fehlgeordnete Kristallgitter. *Schweiz. Mineral. Petrogr. Mitt.* **28**, 456-467.
- LAVES, F. (1935) Zweidimensionale Überstrukturen. *Z. Kristallogr.* **90**, 279-282.
- LONG, R. E. (1965) *The crystal and molecular structures of 7, 7, 8, 8-tetracyanoguinodimethane and cyclopropanecarboxamide and a program for phase determination*. Ph.D. Thesis, University of California, Los Angeles.
- PEACOCK, M. A. (1940) On maucherite (nickel-speiss, placodine, temiskamite). *Mineral. Mag.* **25**, 557-572.
- (1942) Diffuse diffraction and disorder in maucherite. *Amer. Mineral.* **27**, 229.
- YUND, R. A. (1961) Phase relations in the system Ni-As. *Econ. Geol.* **56**, 1273-1296.

*Manuscript received, October 2, 1972; accepted for publication, November 21, 1972.*